



Missouri University of Science and Technology  
Scholars' Mine

International Conferences on Recent Advances  
in Geotechnical Earthquake Engineering and  
Soil Dynamics

1981 - First International Conference on Recent  
Advances in Geotechnical Earthquake  
Engineering & Soil Dynamics

27 Apr 1981, 2:00 pm - 5:00 pm

## Pore Pressure in Silty Sand under Cyclic Shear

R. L. Wei

*Nanjing Hydraulic Research Institute, Nanjing, China*

T. L. Guo

*Nanjing Hydraulic Research Institute, Nanjing, China*

Y. M. Zuo

*Nanjing Hydraulic Research Institute, Nanjing, China*

Follow this and additional works at: <https://scholarsmine.mst.edu/icrageesd>

 Part of the [Geotechnical Engineering Commons](#)

### Recommended Citation

Wei, R. L.; Guo, T. L.; and Zuo, Y. M., "Pore Pressure in Silty Sand under Cyclic Shear" (1981). *International Conferences on Recent Advances in Geotechnical Earthquake Engineering and Soil Dynamics. 2.*  
<https://scholarsmine.mst.edu/icrageesd/01icrageesd/session01b/2>

This Article - Conference proceedings is brought to you for free and open access by Scholars' Mine. It has been accepted for inclusion in International Conferences on Recent Advances in Geotechnical Earthquake Engineering and Soil Dynamics by an authorized administrator of Scholars' Mine. This work is protected by U. S. Copyright Law. Unauthorized use including reproduction for redistribution requires the permission of the copyright holder. For more information, please contact [scholarsmine@mst.edu](mailto:scholarsmine@mst.edu).



# Pore Pressure in Silty Sand under Cyclic Shear

R. L. Wei

Vice Head of Geotech. Eng. Div., Nanjing Hydraulic Research Institute, Nanjing, China.

T. L. Guo & Y. M. Zuo

Engineers, Nanjing Hydraulic Research Institute, Nanjing, China.

**SYNOPSIS** In order to study the liquefaction phenomena of silty sand, saturated specimens prepared in the laboratory according to the dry unit weight of undisturbed samples are used to examine the cyclic shear resistance, pore pressure and residual shear strain developed in these specimens under cyclic loading. These tests are accomplished with a cyclic simple shear test apparatus developed in Nanjing Hydraulic Research Institute. Based on results of these tests expressions of cyclic shear resistance, pore pressure, dynamic shear modulus and residual shear strain as functions of number of cycles, consolidation pressure, initial and cyclic shear stress etc. have been developed.

## INTRODUCTION

Most of the previous liquefaction tests of saturated sands performed in the laboratory dealt with the cyclic shear resistance and various factors controlling the liquefaction characteristics of sands with little consideration of the buildup process of pore pressure under cyclic loading. Since 1975, however, it has been widely recognized that a dynamic response analysis in terms of effective stress is more desirable, and correspondingly a few papers concerning the progressive increase of pore pressure in the sand under cyclic loading have been published (Martin et al., 1975; Seed et al., 1976; Oh-oka, 1976; and others)

During the Tangshan Earthquake on July 28, 1976 there were much physical evidence of soil liquefaction in the medium fine sand backfilled behind the Pier No. 3 of Tianjin New Harbour and in the silty sand deposits on banks of Hai-he R. In order to study the liquefaction behaviour of these deposits, the in-situ standard penetration tests were performed in the above-mentioned sites, and undisturbed sand samples were taken in the same time. After the natural water content and unit weight of these samples had been determined in the field, the disturbed sand materials were transported to the laboratory to be reconstituted and used in the liquefaction tests, during which the buildup process of pore pressure and residual shear strain were also monitored.

## CYCLIC SIMPLE SHEAR TEST APPARATUS

A cyclic simple shear test apparatus has been developed based on the original static simple shear test apparatus in Nanjing Hydraulic Research Institute since 1978 (Zuo, Guo & Wei, 1980). It is composed of four parts---simple shear box, static loading system, electro-magnetic actuator and electronic recording system. The main parts of this apparatus are shown in the left of Fig.1, and the construction of the simple shear box is schematically

illustrated in Fig.2. A specimen with diameter of 7 cm and height of 2 cm is enclosed inside a rubber membrane which is in turn confined by stack of steel rings and attached rigidly to the surfaces of the end plates by tapered sleeves with fastening bolts. It is shown by static test that under an inner pressure of 6 kg/cm<sup>2</sup> the shear box is completely water tight and no membrane inflation appears as there is not any unsupported section of membrane. A pressure transducer is installed at the pedestal of the shear box to measure the pore pressure developed in the specimen during the test. An ancillary device is also provided to apply back pressure through the drainage line. The vertical and horizontal loads are applied pneumatically and controlled separately by two regulator valves. Vertical load is transmitted to the specimen through the load carriage fitted on the top cap of specimen and connected to a horizontally fixed small proving ring. When the horizontal cyclic load is applied, the load carriage is always kept horizontal with minimum rocking by guide ball bearings. The base of the shear box is connected with the loading rams of the horizontal pneumatic loader and electro-magnetic actuator which apply the initial and cyclic shear stress separately. Each of the loading rams is connected with a load cell which monitors the intensity of the load transmitted to the specimen. The pedestal of shear box is mounted on a sliding base with a coefficient of friction of 2% determined by calibration. The magnitude and frequency of excitation is controlled by the extra-low frequency signal generator, the signal generated by the latter is amplified and input to the actuator. The maximum exciting force and stroke of the actuator is 120 kg and 20 mm respectively.

## TEST MATERIAL AND SPECIMEN PREPARATION

Three kinds of test materials---medium fine sand, silty sand and silt had been taken from the above-mentioned sites and tested in the laboratory. Only the test results of silty sand are presented in this paper due to restriction of space. The grain size distribution of



Fig. 1 Cyclic Simple Shear Test Apparatus

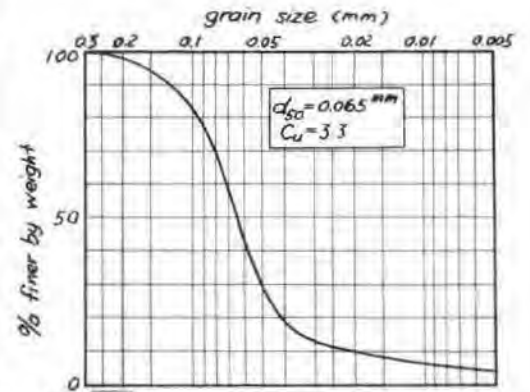


Fig. 3 Grain Size Distribution of Silty Sand.

the silty sand is shown in Fig. 3, and its physico-mechanical properties are as follows; natural unit weight  $\gamma = 2.0 \text{ g/cm}^3$ ; natural water content  $w = 32\%$ ; dry weight  $\gamma_s = 1.52 \text{ g/cm}^3$ ; effective angle of internal friction  $\phi = 23^\circ$ ; number of blows in the standard penetration test = 1-12. In the field the silty sand deposits are embedded at depths of 5.5-7.0 m and 8.5-11.0 m below the ground surface.

Because there are too many fine grains in the silty sand that it is impossible to prepare the saturated specimen by boiling the test material and then pouring it under the water, dry specimen is directly made in the shear box and then saturated by vacuum. The height of the specimen after consolidation is estimated, and the oven-dried silty sand is weighed, poured into a membrane inside the shear box, and tapped in layers to get the required density (the dry unit weight after consolidation =  $1.52 \pm 0.02 \text{ g/cm}^3$ ).

After the dry specimen has been prepared, the air tight cell is mounted outside the shear box as shown in the right of Fig. 1. The valve of drainage line on the base of specimen is closed at first, and vacuum is applied from the top of the cell for 15 minutes. The valve is then opened slightly to let the water filtrating slowly through the specimen from the base until the water level in the cell has raised over the top surface of the specimen, and the vacuum is henceforth maintained for 10 minutes again. Caution must be taken that the filtration of water through the specimen should not be too rapid in order to avoid the disturbance of the

placement structure of the specimen. It is shown by test that the degree of saturation of the specimen prepared with this procedure is generally high than 97%.

After the specimen has been saturated, the air tight cell is dismounted, and the top cap is put on the surface of specimen. A special holder is constructed for the cap, allowing it to be lowered gently onto the specimen. When the rubber membrane is rolled and attached to the cap with tapered sleeve and fastening bolt, the cap is fixed temporarily to the holder, thereby preventing any vertical movement of cap and disturbance of the prepared specimen. When the vertical pressure  $\sigma_{vc}$  has been applied to the specimen, the induced pore pressure  $u$  is monitored before the drainage begins in order to check the degree of saturation of specimen. If the value of pore pressure coefficient  $B$  is less than 0.98, back pressure may be applied to the specimen to increase the degree of saturation. Moreover, initial shear stress  $\tau_0$  may also be applied to the specimen with the horizontal pneumatic loader when it is necessary, and the specimen will be consolidated under the combined action of vertical pressure and horizontal shear stress.

When the consolidation of the specimen has completed, the drainage valve is closed, and the cyclic sinusoidal shear stress with a frequency of 2 Hz is applied by the electro-magnetic actuator. During the test the variations of cyclic shear stress, shear strain and pore pressure are measured by the transducers and recorded by the oscilloscope. Some typical time histories of these variables recorded are shown in Fig. 4, where (a) and (b) represents the record in case of  $\tau_0 = 0$  and  $\tau_0 > 0$  respectively.

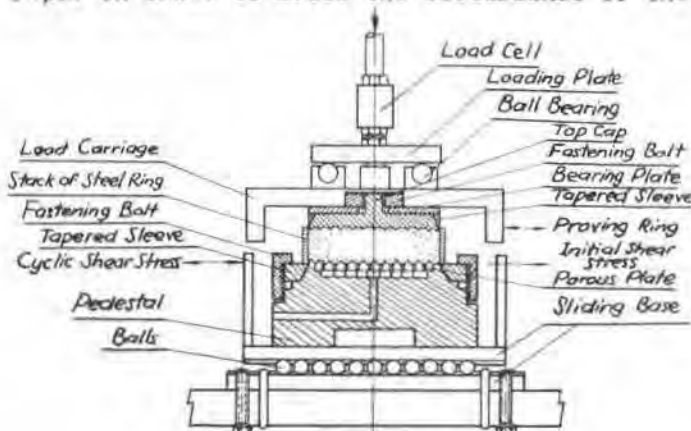


Fig. 2 Simple Shear Box

#### CYCLIC SHEAR RESISTANCE

It is shown that the responses of specimens with and without initial shear stress are remarkably different (Fig. 4). In cases of  $\tau_0 = 0$  the specimens usually liquefy suddenly after a certain number of stress cycles. At the early stage of the test the pore pressure in the specimen builds up gradually. Once some critical point is reached, the pore pressure increases suddenly until its peak value equals to the externally applied vertical pressure ( $u_{\max} = \sigma_{vc}$ ), i.e. the initial liquefaction is induced. In cases of  $\tau_0 > 0$  the pore pressure as well as the residual shear

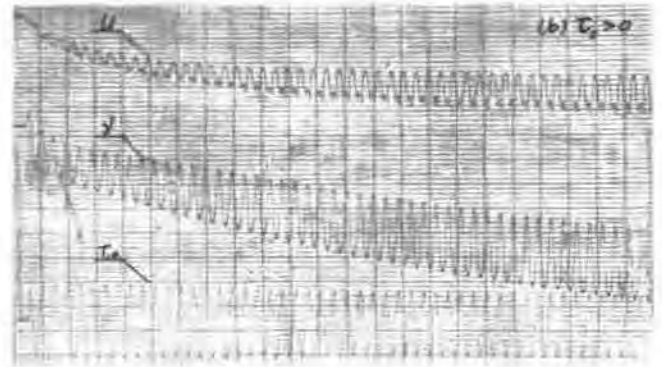
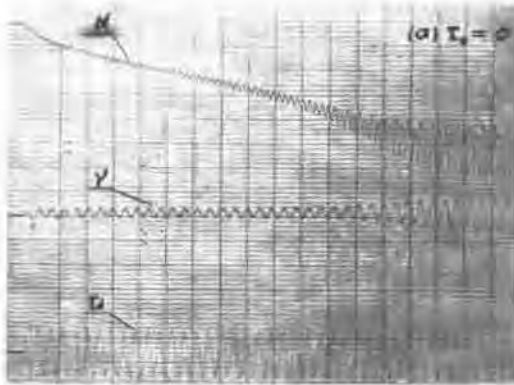


Fig. 4 Recorded Time Histories of Cyclic Stress, Shear Strain and Pore Pressure.

strain increases gradually. However, as some critical point is reached, the rate of increase of pore pressure would be slowed down rather than accelerated, and the pore pressure would eventually remains unchanged on some value. That is to say, in the latter cases the pore pressure would not develop to such high value as to induce initial liquefaction at which the effective stress reduces to zero, i.e.  $u_{max} < \sigma_{vc}$  in cases of  $\tau_0 > 0$ , and the specimen might be considered to have failed only when the residual shear strain becomes excessive.

The relationships between the cyclic shear resistance and the number of stress cycles required to cause initial liquefaction under various stress conditions in cases of  $\tau_0 = 0$  are shown in Fig. 5. It is evident from this figure that for the silty sand of given grain size characteristics and density, the higher the consolidation pressure, the larger the cyclic shear resistance. If the cyclic shear resistance is normalized with respect to the consolidation pressure, then all the test points fall in the vicinity of a mean curve as shown in Fig. 6(a).

As mentioned above, in cases of  $\tau_0 > 0$  the initial liquefaction will not be reached. When we study the development of pore pressure and residual shear strain with increasing number of cycles, however, it is sometimes convenient to normalize the number of stress cycles with some reference number of cycles which implies the onset of certain critical state of the specimen. It is shown that as the pore pressure in the specimen induced under cyclic loading eventually remains unchanged in cases of  $\tau_0 > 0$ , the residual shear strain has in general increased to a value greater than 5%. Therefore it is considered that the specimen at this instant has reached a so called "ultimate" state at which

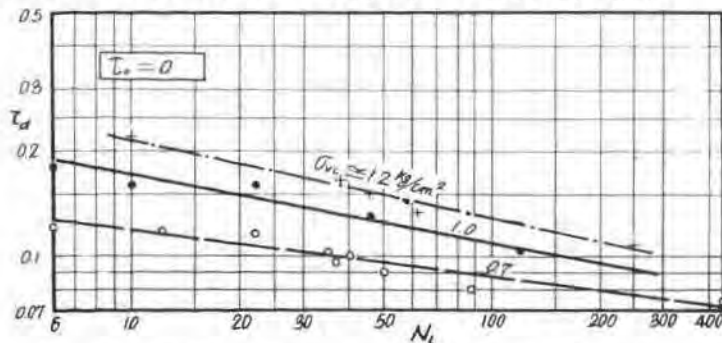


Fig. 5 Cyclic Stress versus Number of Cycles

the dynamic strength of the specimen has been nearly exhausted. The corresponding number of cycles is defined as the "ultimate" number of cycles  $N_1$ . Then the cyclic shear stress ratio is plotted versus the "ultimate" number of cycles defined in this way as shown in Fig. 6(b). It is evident that all test points with various initial shear stress also fall in the vicinity of the experimental curve obtained in cases of  $\tau_0 = 0$  except those of  $N_1 < 15$ . Consequently the cyclic shear resistance of all these test, including both cases of  $\tau_0 = 0$  and  $\tau_0 > 0$  may be unifiedly expressed as follows (except those of  $N_1 < 15$  for  $\tau_0 > 0$  whose cyclic shear resistance are somewhat higher):

$$\tau_d / \sigma_{vc} = FN_1^{-b} \quad (1)$$

where  $F$  and  $b$  are empirical coefficients, for the silty sand tested,  $F = 0.23$  and  $b = 0.144$ .

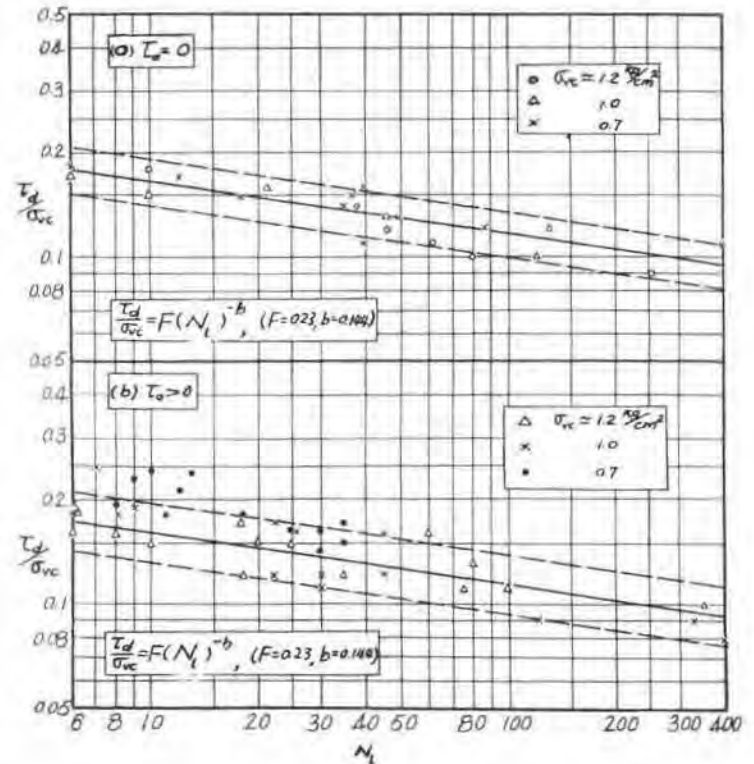


Fig. 6 Cyclic Stress Ratio versus Number of Cycles

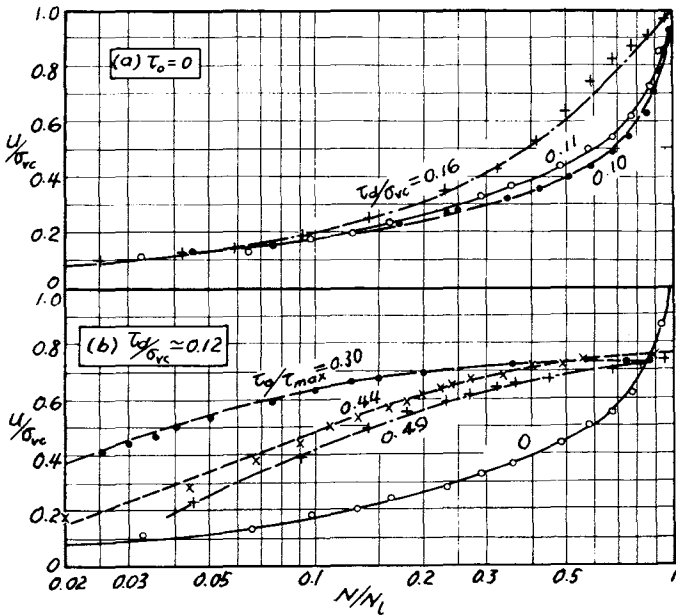


Fig. 7 Pore Pressure versus Cycles Ratio.

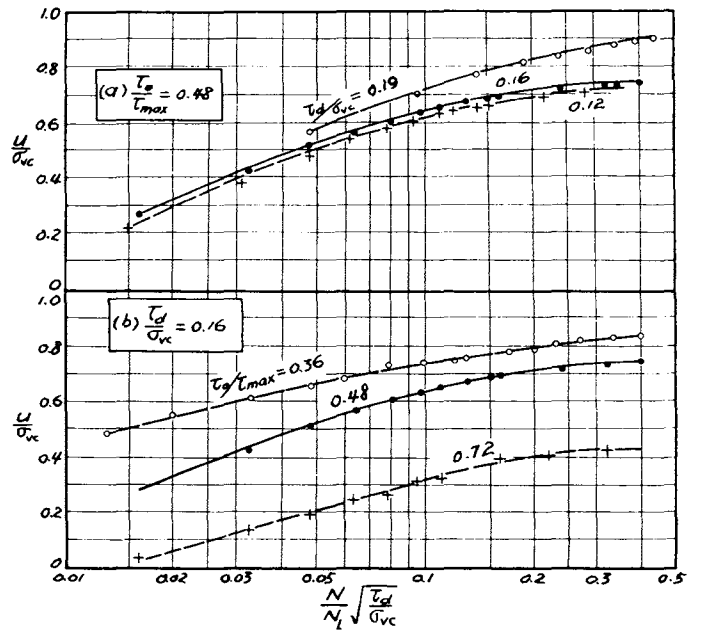


Fig. 8 Pore Pressure Ratio versus Factor of Dynamic Effect

PORE PRESSURE

Some typical test results of  $\tau_0 = 0$  are shown in Fig. 7(a). It is seen from this figure that even if the pore pressure  $u$  and number of cycles  $N$  is normalized with respect to  $\sigma_{vc}$  and  $N_1$  respectively, single curve as that shown in Fig. 6 is not obtained. The cycles ratio  $N/N_1$  required to cause equal value of pore pressure ratio  $u/\sigma_{vc}$  varies with the cyclic shear stress ratio  $\tau_d/\sigma_{vc}$ , and the higher the cyclic shear stress ratio, the smaller the cycles ratio required to induce a given value of pore pressure ratio. However, if the values of pore pressure ratio are plotted against the corresponding values of factor of dynamic effect  $r_d$  which is defined as

$$r_d = (N/N_1) \sqrt{\tau_d/\sigma_{vc}}$$

expressing the combined influence of the amplitude and number of cycles of the dynamic stress, then the test points fall closely in the vicinity of a mean curve as shown in Fig. 9(a). Some typical test results of  $\tau_0 > 0$  are shown in Fig. 7(b). It is seen that the development of pore pressure in cyclic loading tests with initial shear stress is remarkably different from that of  $\tau_0 = 0$ , hence the test data of these two cases would rather be interpreted separately.

When the test results of  $\tau_0 > 0$  are plotted by the same procedure as that used in Fig. 9(a), it is seen that (Fig. 8) the higher the initial shear stress level  $\tau_0/\tau_{max}$  (where  $\tau_{max}$  is the static drained shear strength of silty sand under the corresponding  $\sigma_{vc}$ , i.e.  $\tau_{max} = \sigma_{vc} \tan \phi' + c'$ ), the smaller the pore pressure ratio induced under the same dynamic effect ( $r_d = \text{const.}$ ); and under the same initial shear stress level, the higher the cyclic shear stress ratio, the higher the induced pore pressure ratio, although the influence of cyclic stress is smaller than that of the initial stress. If the values of pore pressure ratio are divided by a factor

$$M = 1 - \frac{h}{\tau_d/\sigma_{vc}} (\tau_0/\tau_{max})^d$$

and plotted versus values of factor of dynamic effect, then for each of the cases of  $\tau_0/\tau_{max} < 0.16$  and  $\tau_0/\tau_{max} \geq 0.16$  a mean curve may be drawn as shown in Fig. 9(b). The factor  $M$  reflects mainly the influence of initial shear stress, and  $h$  and  $d$  in the above expression are empirical coefficients, for the silty sand tested,  $h=0.1$  and  $d=2$ .

The curves in Fig. 9 represent the development of pore pressure with increasing number of stress cycles in cases of  $\tau_0 = 0$  and  $\tau_0 > 0$  respectively, and may be expressed unifiedly by the following empirical relationship:

$$u/\sigma_{vc} = CM(r_d)^a \quad (2)$$

where  $C$  and  $a$  are empirical coefficients, for the silty sand tested, their values are listed in Table I; and the definitions of the other notations are same as above.

Table I Values of Coeff. in Formula (2)

$\tau_0/\tau_{max}$	=0		< 0.16		≥ 0.16	
	≤ 0.225	> 0.225	≤ 0.2	> 0.2	≤ 0.08	> 0.08
C	1.15	5.0	1.5	3.2	3.6	1.3
a	0.56	1.55	0.60	1.09	0.65	0.245

Values of the coefficients shown in Table I reflect different trends of development of pore pressure under various initial stress conditions. In cases of  $\tau_0 = 0$ , the value of  $a$  is small at first and then becomes larger, indicating the fact that the pore pressure increases gradually in the early stage of test, and once it reaches a value equal



to 50% of the consolidation pressure, it increases abruptly up to initial liquefaction. In cases of  $\tau_0 > 0$  when  $\tau_0/\tau_{max} \geq 0.16$ , the value of  $\tau_0/\tau_{max}$  is at first somewhat larger and then becomes much smaller than that in cases of  $\tau_0 = 0$ , indicating that in the early stage of these tests the rate of buildup of pore pressure is somewhat quicker than that in cases of  $\tau_0 = 0$ , and once the pore pressure becomes to equal to 70% of its maximum value, it increases slowly and eventually remains unchanged on certain value. When  $0 < \tau_0/\tau_{max} < 0.16$  the variation of pore pressure may be regarded as the intermediate transition between those of the cases of  $\tau_0 = 0$  and  $\tau_0/\tau_{max} \geq 0.16$  as shown by the broken line in Fig. 9(b).

where  $G_0 = k\sqrt{\sigma_{vc}}$ , for the silty sand tested  $k=40$ ;  $m$ ,  $n$  and  $t$  are empirical coefficients whose values for the silty sand tested are listed in Table II(a) and II(b).

Table II(a) Values of Coeff. in Formula (3) for  $\tau_0 = 0$

$\tau_d/\sigma_{vc}$	$\leq 0.15$		$> 0.15$		
	$N/N_1$	$0-0.875$	$0.875-1$	$0-0.4$	$0.4-1$
$m$		1	1.5	1	3.2
$n$		0.6	85	5.6	14.5
$t$		0	0.875	0	0.4

Table II(b) Values of Coeff. in Formula (3) for  $\tau_0 > 0$

$\tau_0/\tau_{max}$	$< 0.16$	$0.16-0.4$	$> 0.4$	$< 0.16$	$0.16-0.4$
	$\tau_d/\sigma_{vc}$	$\leq 0.125$	$\leq 0.15$	-	$> 0.125$
$N/N_1$		$0-0.9$	$0.9-1$	$0-0.2$	$0.2-1$
$m$		1	2	1	1.22
$n$		1.1	5	1.1	4
$t$		0	0.9	0	0.2

DYNAMIC SHEAR MODULUS AND RESIDUAL SHEAR STRAIN

The dynamic shear modulus at any cycle  $G_N = \tau_d / \gamma_{dN}$  calculated from the test results is at first normalized with respect to the initial shear modulus  $G_0$ , and plotted against the cycles ratio  $N/N_1$  as shown in Fig. 10. It is evident that, in cases of  $\tau_0 = 0$ , at smaller values of cyclic shear stress ratio ( $\tau_d/\sigma_{vc} \leq 0.15$ ), the test points are concentrated to a mean curve composed of two straight lines, and at larger values of cyclic shear stress ratio ( $\tau_d/\sigma_{vc} > 0.15$ ), a mean curve is still obtainable as shown by broken line in Fig. 10(a), even though the test points are relatively scattering. Similarly, for cases of  $\tau_0 > 0$ , two mean curves are obtained for different conditions as shown in Fig. 10(b). These curves in Fig. 10 may also be unifiedly expressed by the following equation:

$$1/G_N = [m + n(N/N_1 - t)]/G_0 \quad (3)$$

In cases of  $\tau_0 > 0$  the cyclic shear stress induces in the specimen cyclic shear strain as well as residual shear strain, both of them increase with increasing number of cycles. Based on the results of the above-mentioned cyclic shear tests of  $\tau_0 > 0$ , the development of residual shear strain of silty sand under cyclic loading is described as follows.

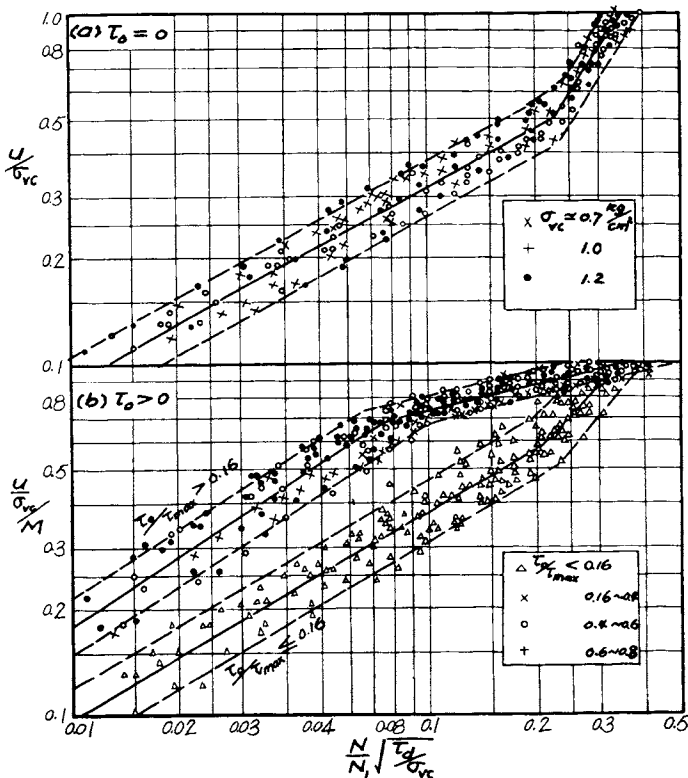


Fig. 9 Modified Pore Pressure Level versus Factor of Dynamic Effect.

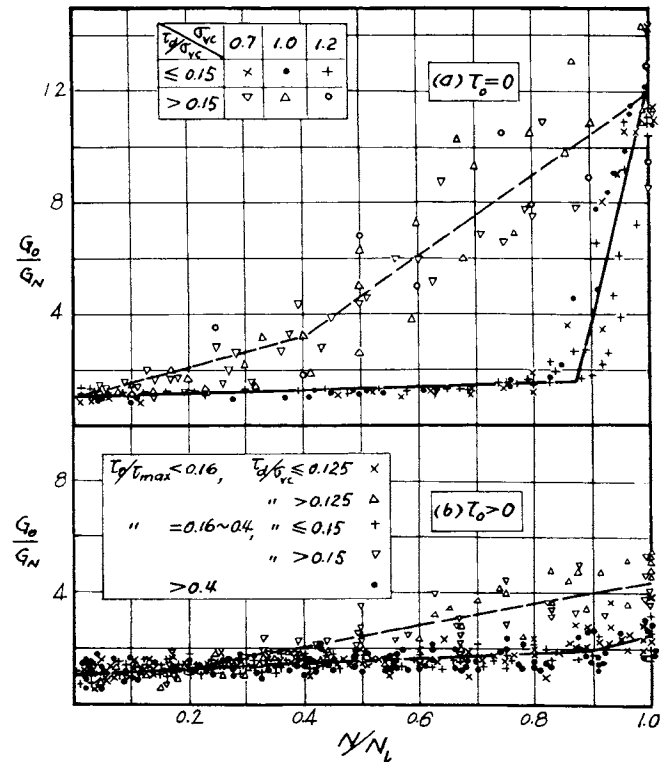


Fig. 10 Dynamic Shear Modulus Ratio versus Cycles Ratio.

Table III(a) Values of Coeff. in Formula(4) for  $\tau_o/\tau_{max} \geq 0.16$ .

$\tau_d/\sigma_{vc}$	$\leq 0.15$		$> 0.15$	
	0-0.25	0.25-1	0-0.2	0.2-1
p	1	12	1	18
q	44	26.7	35	22.5
s	0	0.25	0	0.2

Table III(b) Values of Coeff. in Formula(4) for  $\tau_o/\tau_{max} < 0.16$

$\tau_d/\sigma_{vc}$	0.075-0.100		0.100-0.125		$> 0.125$	
	0-0.8	0.8-1	0-0.7	0.7-1	0-0.6	0.6-1
p	1	4.3	1	4.85	1	5.4
q	5.5	70	5.5	50	5.5	30
s	0	0.8	0	0.7	0	0.6

In order to normalize the residual shear strain a reference shear strain defined as initial cyclic shear strain  $\gamma_{d0} = \tau_d/G_o$  is introduced at first. Then the normalized residual shear strain  $\gamma_r/\gamma_{d0}$  multiplied by the above-mentioned influence factor of initial shear stress M are plotted against the cycles ratio  $N/N_1$  as shown in

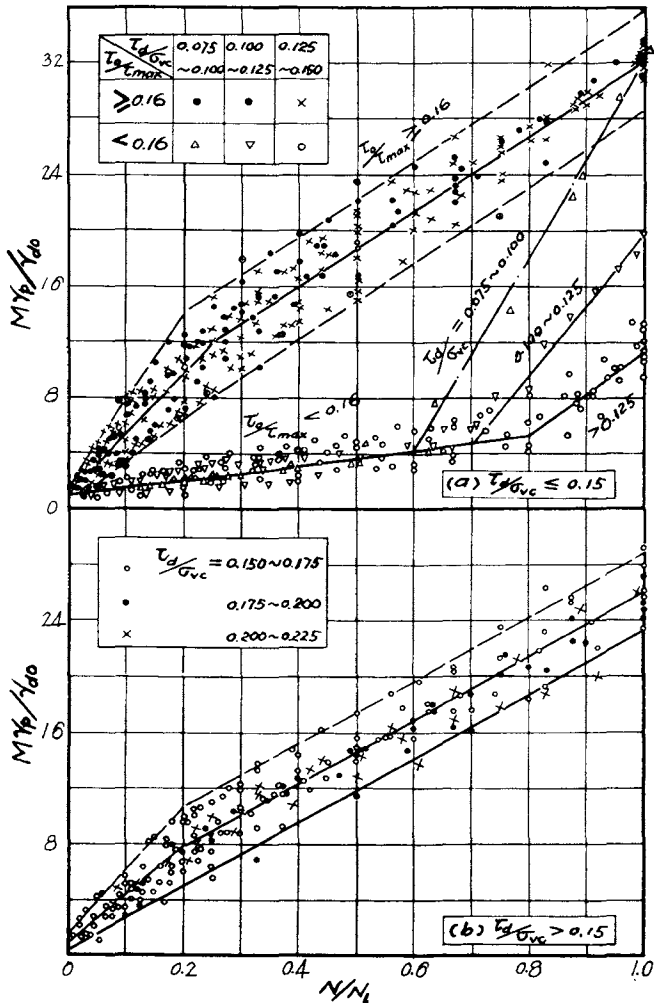


Fig. 11 Residual Shear Strain Ratio versus Cycles Ratio.

Fig. 11. It is evident that, when  $\tau_o/\tau_{max} \geq 0.16$  for each of the cases of  $\tau_d/\sigma_{vc} \leq 0.15$  and  $\tau_d/\sigma_{vc} > 0.15$  a mean curve may be drawn. As an intermediate transition between the cases of  $\tau_o = 0$  and  $\tau_o/\tau_{max} \geq 0.16$  again, the test points of  $\tau_o/\tau_{max} < 0.16$  fall on three different curves for various values of  $\tau_d/\sigma_{vc}$  as shown in the lower part of Fig. 11(a). Nevertheless, the residual shear strain at any number of cycles before the initial liquefaction or "ultimate" state is reached may be unifiedly expressed by the following equation:

$$\gamma_p = \gamma_{d0} [p + q(N/N_1 - s)] / M \quad (4)$$

where p, q and s are the empirical coefficients whose values for silty sand tested under various stress conditions are listed in Tables III(a) and III(b).

CONCLUDING REMARKS

The test data presented here are those among the first sets of results obtained with the cyclic simple shear test apparatus developed in Nanjing Hydraulic Research Institute which has just been operated since the end of 1979. Although the amount of data is not quite sufficient and somewhat scattering, the empirical relationships obtained seem reasonable, and may be used in the dynamic response analysis of earth bank and retaining wall in terms of effective stress (e.g. Wei, 1981). These are doubtless tentative results and might be not generally valid. However, the forms of these relationships are similar to those of medium fine sand obtained from the cyclic triaxial tests (Wei, 1978). Hence they might be used to determine at least qualitatively the influences of some important factors, and this would be significant for further studying the mechanism of development of pore pressure and residual shear strain of silty sand under the cyclic loading.

REFERENCES

Martin, G.R., W.D.L. Finn & H.B. Seed (1975), "Fundamentals of Liquefaction under Cyclic Loading". Proc ASCE, Vol.101, No.GT5, p.423.

Oh-oka, H. (1976), "Drained and Undrained Stress-Strain Behaviour of Sands Subjected to Cyclic Shear Stress under Nearly Plane Strain Condition". Soil and Foundation, Vol.16, No.3, p.19.

Seed, H.B., G.R. Martin & J. Lysmer (1976), "Pore Pressure Change during Soil Liquefaction". Proc. ASCE, Vol.102, No. GT4, p.323.

Wei, R.L. (1978), "The Cyclic Shear Resistance & Pore Pressure in the Saturated Sand under Cyclic Loading". Report No.7812, Nanjing Hydraulic Research Institute.

Wei, R.L. (1981), "The Local Amplification of the Seismic Accelerations in the Vicinity of the Crest of Bank Slope". Proc. 3rd Chinese National Conference on Soil Mechanics & Foundation Engineering (in the press).

Zuo, Y.M., J.L. Guo & R.L. Wei (1980), "A Cyclic Simple Shear Test Apparatus". Chinese Journal of Geotech. Eng. Vol.2, No.1, p.78.